Consequences of CP transformed mixed ν_μ-ν_τ antisymmetry

Probir Roy

Centre for Astroparticle Physics and Space Science
Bose Institute, Kolkata

DAE HEP 2018, IITM

Collaborators R. Sinha and A. Ghosal of SINP

PLAN OF THE TALK

- INTRODUCTION
- NEUTRINO MIXING ANGLES AND PHASES
- NUMERICAL ANALYSIS
- NEUTRINOLESS DOUBLE BETA DECAY
- CP ASYMMETRY IN OSCILLATIONS
- FLAVOR FLUX RATIOS AT NEUTRINO TELESCOPES
- CONCLUSION

Statement of $CP^{\theta\mu\tau A}$: $\mathcal{G}^\theta M_\nu \mathcal{G}^\theta = -M_\nu^*$ Sinha, Roy, Ghosal (2018)

under $\nu_{L\ell} \to i\mathcal{G}^\theta_{lm}\gamma^0\nu^C_{Lm}$

with generator $$\mathcal{G}^\theta = i\begin{pmatrix} -1 & 0 & 0 \\ 0 & -\cos\theta & \sin\theta \\ 0 & \sin\theta & \cos\theta \end{pmatrix}.$$

Mixing angle $\theta \in [0, \pi/2]$ with $\theta = \pi/2 \leftrightarrow$ exact CP transformed $\nu_\mu\nu_\tau$ antisymmetry. Most general form of M_ν is

$$M_\nu^{CP\theta A} = \begin{pmatrix} ix & a_1 + ia_2 & a_1 t_{\frac{\theta}{2}}^{-1} - ia_2 t_{\frac{\theta}{2}} \\ a_1 + ia_2 & y_1 + iy_2 & y_1 c_\theta s_\theta^{-1} + ic \\ a_1 t_{\frac{\theta}{2}}^{-1} - ia_2 t_{\frac{\theta}{2}} & y_1 c_\theta s_\theta^{-1} + ic & -y_1 + i(y_2 + 2cc_\theta s_\theta^{-1}) \end{pmatrix}$$

with 7 real parameters $x, a_{1,2}, c, y_{1,2}, \theta$. Here $c_\theta \equiv \cos\theta, s_\theta \equiv \sin\theta$, $t_{\frac{\theta}{2}} \equiv \tan\frac{\theta}{2}$.

Lam's observation: Lam (2007)

$$\mathcal{G}^\theta U^* = U\tilde{d}, \quad \tilde{d} = \mathrm{diag}(\tilde{d}_1, \tilde{d}_2, \tilde{d}_3), \ d_{1,2,3} = \pm 1.$$

$$U = \mathrm{diag}(e^{i\phi_1}, e^{i\phi_2}, e^{i\phi_3}) U_{\mathrm{PMNS}},$$

$$U_{\mathrm{PMNS}} = \begin{pmatrix} c_{12}c_{13} & e^{i\frac{\alpha}{2}} s_{12}c_{13} & s_{13}e^{-i(\delta-\frac{\beta}{2})} \\ -s_{12}c_{23} - c_{12}s_{23}s_{13}e^{i\delta} & e^{i\frac{\alpha}{2}}(c_{12}c_{23} - s_{12}s_{13}s_{23}e^{i\delta}) & c_{13}s_{23}e^{i\frac{\beta}{2}} \\ s_{12}s_{23} - c_{12}s_{13}c_{23}e^{i\delta} & e^{i\frac{\alpha}{2}}(-c_{12}s_{23} - s_{12}s_{13}c_{23}e^{i\delta}) & c_{13}c_{23}e^{i\frac{\beta}{2}} \end{pmatrix}.$$

Algebraic matching leads to

$$e^{i\alpha} = \tilde{d}_1\tilde{d}_2, \ e^{2i(\delta-\frac{\beta}{2})} = \tilde{d}_1\tilde{d}_3$$

$$\Rightarrow \alpha = 0 \text{ or } \pi, \text{ and } \beta = 2\delta \text{ or } 2\delta - \pi.$$

Moreover, $\cot 2\theta_{23} = \cot\theta \cos(\phi_2 - \phi_3)$, $\sin\delta = \pm \sin\theta / \sin 2\theta_{23}$, i.e. $\theta \to \pi/2 \Rightarrow \theta_{23} \to \frac{\pi}{4}$. In general, $\theta_{23} \neq \pi/4$ and $\delta \neq 0$ or π.

3.NUMERICAL ANALYSIS

Input mixing angles and mass-squared differences from latest global analysis. Esteban et al (2017)

Neutrino mass sum $m_1 + m_2 + m_3 < 0.17$ eV from Planck data. Aghanim et al (2016)

Table: Input 3σ ranges used in the analysis

Values	θ_{12} degrees	θ_{23} degrees	θ_{13} degrees	Δm^2_{21} 10^{-5}eV^2	$\lvert\Delta m^2_{31}\rvert$ $10^{-3}(\text{eV}^2)$
NO	31.42 to 36.05	40.3 to 51.5	8.09 to 8.98	6.80 to 8.02	2.399 to 2.593
IO	31.43 to 36.06	41.3 to 51.7	8.14 to 9.01	6.80 to 8.02	2.399 to 2.593

Table: Output values of the parameters of M_ν

Values	$10^3 x$	$10^3 a_1$	$10^3 a_2$	$10^3 y_1$	$10^3 y_1$	$10^3 c$	$\theta(^\circ)$
NO	-22 to 22	-45 to 45	-32 to 32	-35 to 35	-45 to 45	-35 to 35	12 to 164
IO	-25 to 25	-45 to 45	-4 to 4	-25 to 25	-35 to 35	-25 to 25	2 to 156

Table: Predictions on the light neutrino masses.

Normal Ordering ($m_3 > m_2$)			Inverted Ordering ($m_3 < m_1$)		
$10^3 m_1(\mathrm{eV})$	$10^{-3} m_2(\mathrm{eV})$	$10^3 m_3(\mathrm{eV})$	$10^3 m_1(\mathrm{eV})$	$10^3 m_2(\mathrm{eV})$	$10^3 m_3(\mathrm{eV})$
$8.4 \times 10^{-2} - 49$	$9 - 51$	$50 - 71$	$48 - 64$	$49 - 66$	$4.4 \times 10^{-2} - 42$

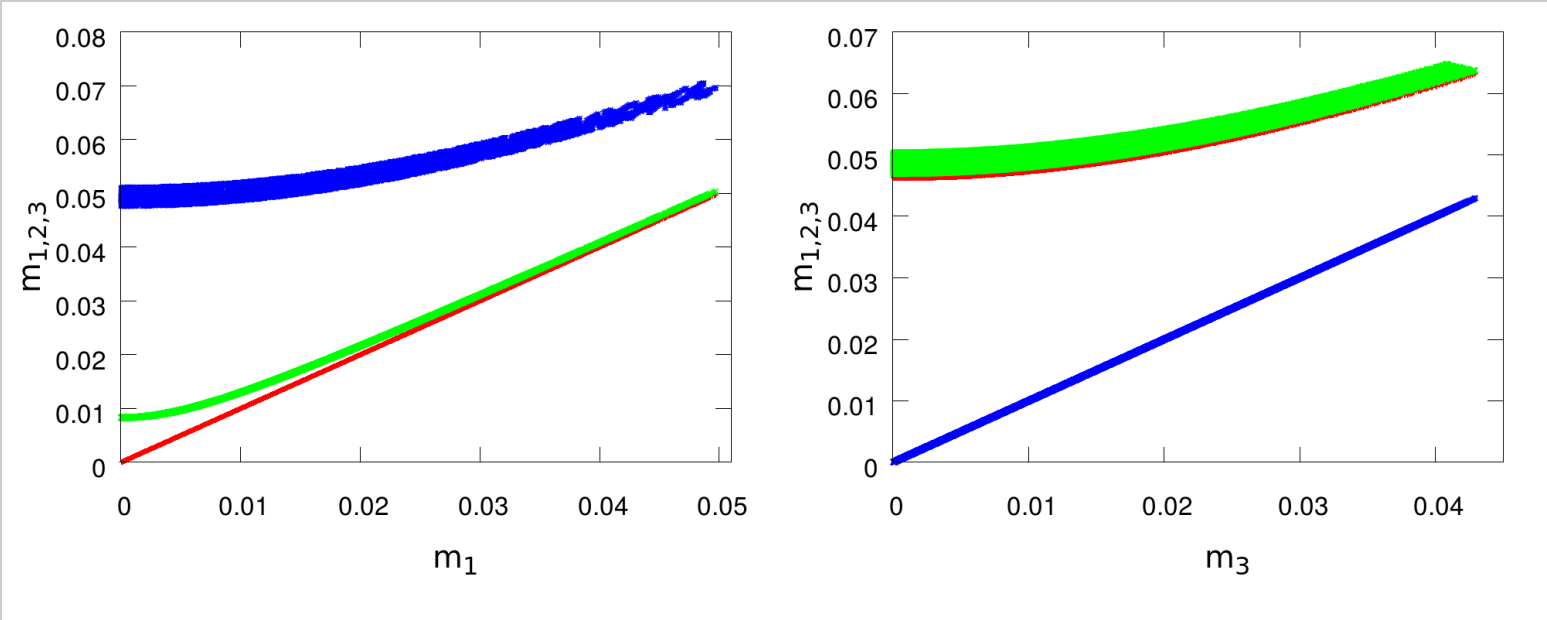

Neutrino masses for normal (left) and inverted (right) ordering against the lightest mass eigenvalue. The red, green and blue bands refer to m_1, m_2 and m_1 respectively.

$$(A, Z) \rightarrow (A, Z+2) + 2e^-$$

Half-life $T^{0\nu}_{1/2} = G_{0\nu}|\mathcal{M}|^2|M^{ee}_\nu|^2 m_e^{-2}$,
$G_{0\nu}$ = two-body phase space factor, $\mathcal{M}$ = nuclear matrix element,

$$M^{ee}_\nu = c^2_{12}c^2_{13}m_1 + s^2_{12}c^2_{13}m_2 e^{i\alpha} + s^2_{13}m_3 e^{i(\beta-2\delta)}$$

Four cases in our model.
(i) $|M^{ee}_\nu| = c^2_{12}c^2_{13}m_1 + s^2_{12}c^2_{13}m_2 + s^2_{13}m_3$ for $\alpha = 0, \beta = 2\delta$,

(ii)$|M^{ee}_\nu| = c^2_{12}c^2_{13}m_1 + s^2_{12}c^2_{13}m_2 - s^2_{13}m_3$ for $\alpha = 0, \beta = 2\delta - \pi$,

(iii) $|M^{ee}_\nu| = c^2_{12}c^2_{13}m_1 - s^2_{12}c^2_{13}m_2 + s^2_{13}m_3$ for $\alpha = \pi, \beta = 2\delta$ and

(iv) $|M^{ee}_\nu| = c^2_{12}c^2_{13}m_1 - s^2_{12}c^2_{13}m_2 - s^2_{13}m_3$ for $\alpha = \pi, \beta = 2\delta - \pi$.

Plots of $|M_\nu^{ee}|$ versus the minimum neutrino mass m_{min}

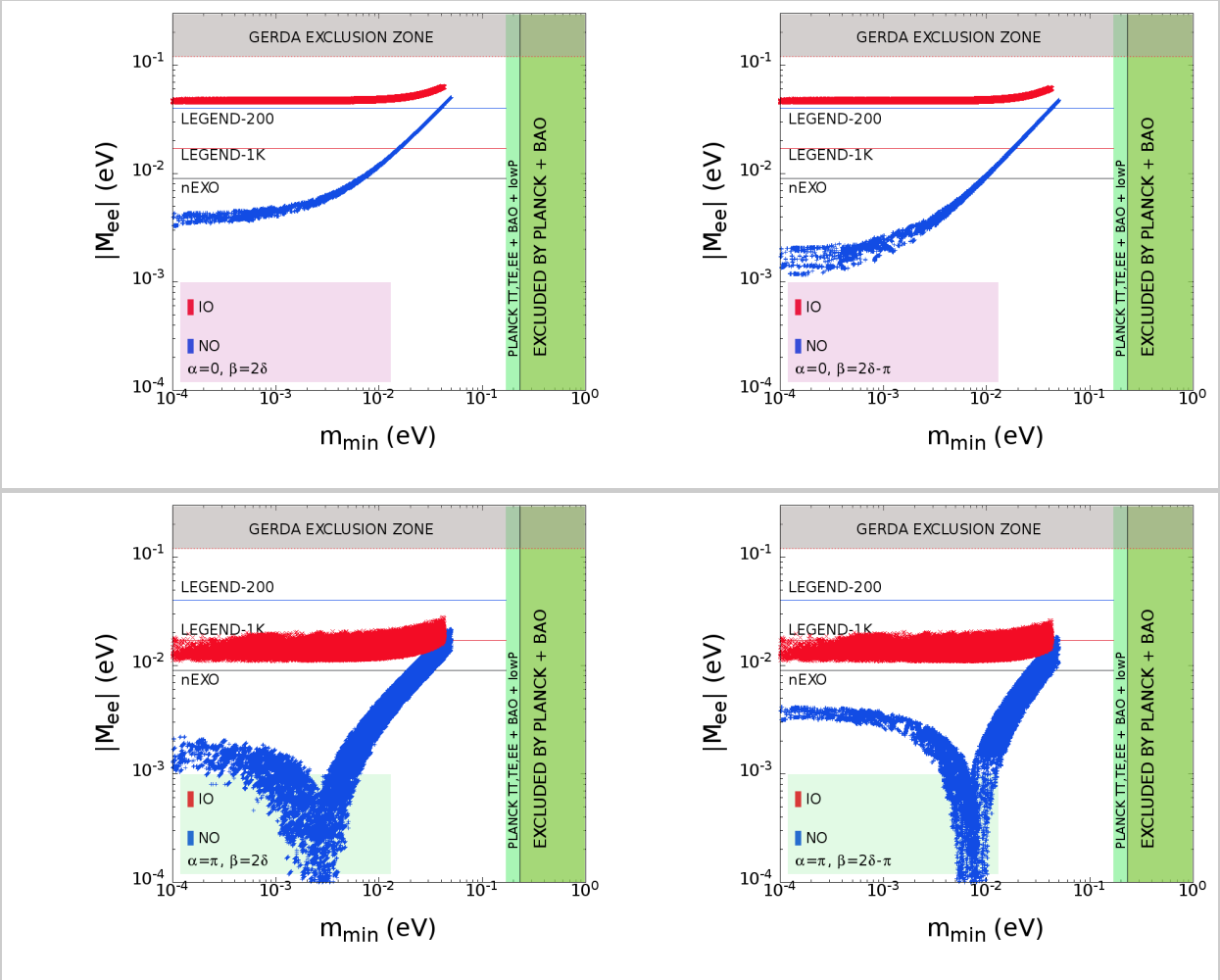

The four plots correspond to four possible choices of α and β.

Predicted signal below the reach of GERDA phase II but reachable by LEGEND-200, LEGEND-1K and nEXO. Failure of nEXO to see any signal would rule out our model for IO.

Experimental CP asymmetry

$$A_{\mu e} \equiv \frac{P(\nu_\mu \to \nu_e) - P(\bar{\nu}_\mu \to \bar{\nu}_e)}{P(\nu_\mu \to \nu_e) + P(\bar{\nu}_\mu \to \bar{\nu}_e)} = \frac{2\sqrt{P_{31}}\sqrt{P_{21}} \sin\Delta_{32} \sin\delta}{P_{31} + P_{21} + 2\sqrt{P_{31}}\sqrt{P_{21}} \cos\Delta_{32} \cos\delta}$$

with

$$\sqrt{P_{31}} \simeq s_{23} \sin 2\theta_{13} \frac{\sin(\Delta_{31} - aL)}{\Delta_{31} - aL} \Delta_{31},$$

$$\sqrt{P_{21}} \simeq c_{23} \sin 2\theta_{12} \frac{\sin(aL)}{aL} \Delta_{21},$$

$\Delta_{ij} = \frac{\Delta m^2_{ij} L}{4E}$, $a = \frac{G_F N_e}{\sqrt{2}} \simeq 3500\mathrm{km}^{-1}$, $N_e =$ electron density in the medium

$\sin\delta$ and $\cos\delta$ can have four different combinations.

Table: Four possibilities for $A_{\mu e}$

Possibilities	$\sin\delta$	$\cos\delta$
Case A	$+\sin\theta(\sin 2\theta_{23})^{-1}$	$+(\sin 2\theta_{23})^{-1}\sqrt{\cos^2\theta \sin^2 2\theta_{23} - \sin^2\theta \cos^2 2\theta_{23}}$
Case B	$-\sin\theta(\sin 2\theta_{23})^{-1}$	$+(\sin 2\theta_{23})^{-1}\sqrt{\cos^2\theta \sin^2 2\theta_{23} - \sin^2\theta \cos^2 2\theta_{23}}$
Case C	$+\sin\theta(\sin 2\theta_{23})^{-1}$	$-(\sin 2\theta_{23})^{-1}\sqrt{\cos^2\theta \sin^2 2\theta_{23} - \sin^2\theta \cos^2 2\theta_{23}}$
Case D	$-\sin\theta(\sin 2\theta_{23})^{-1}$	$-(\sin 2\theta_{23})^{-1}\sqrt{\cos^2\theta \sin^2 2\theta_{23} - \sin^2\theta \cos^2 2\theta_{23}}$

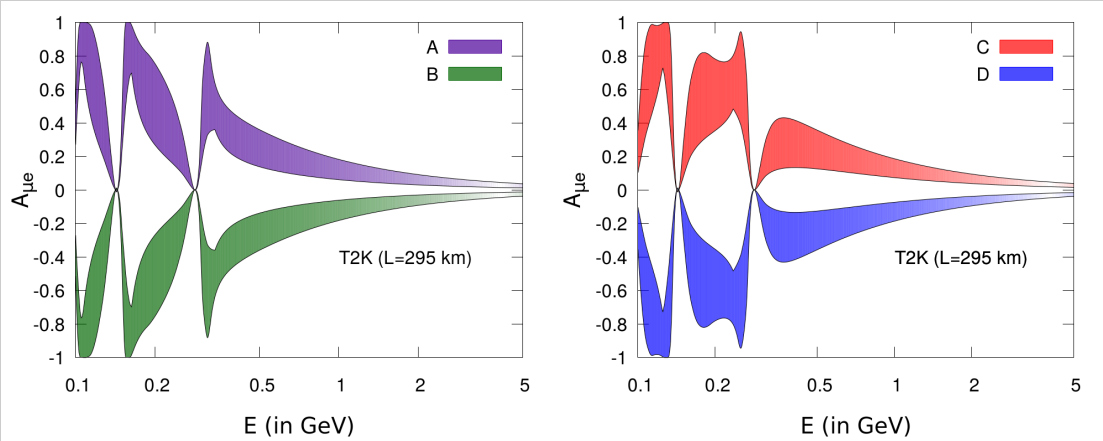

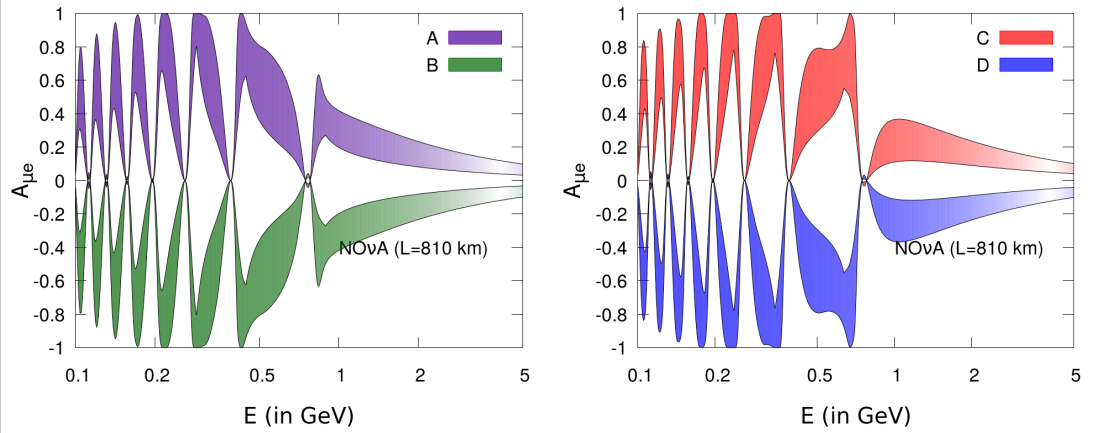

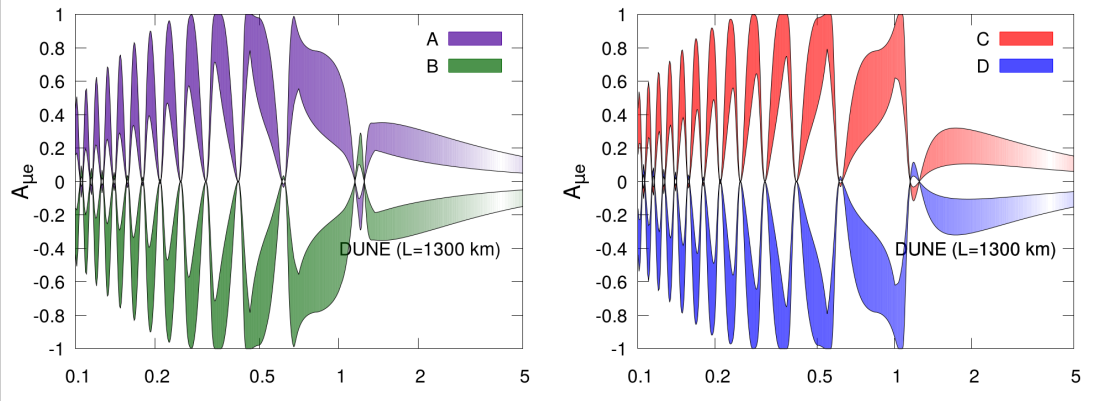

Plots of $A_{\mu e}$ against beam energy E for different baselines lengths of T2K, NOνA and DUNE respectively.

The numerical distinction between NO and IO is insignificant for the 3σ range of θ_{23}.

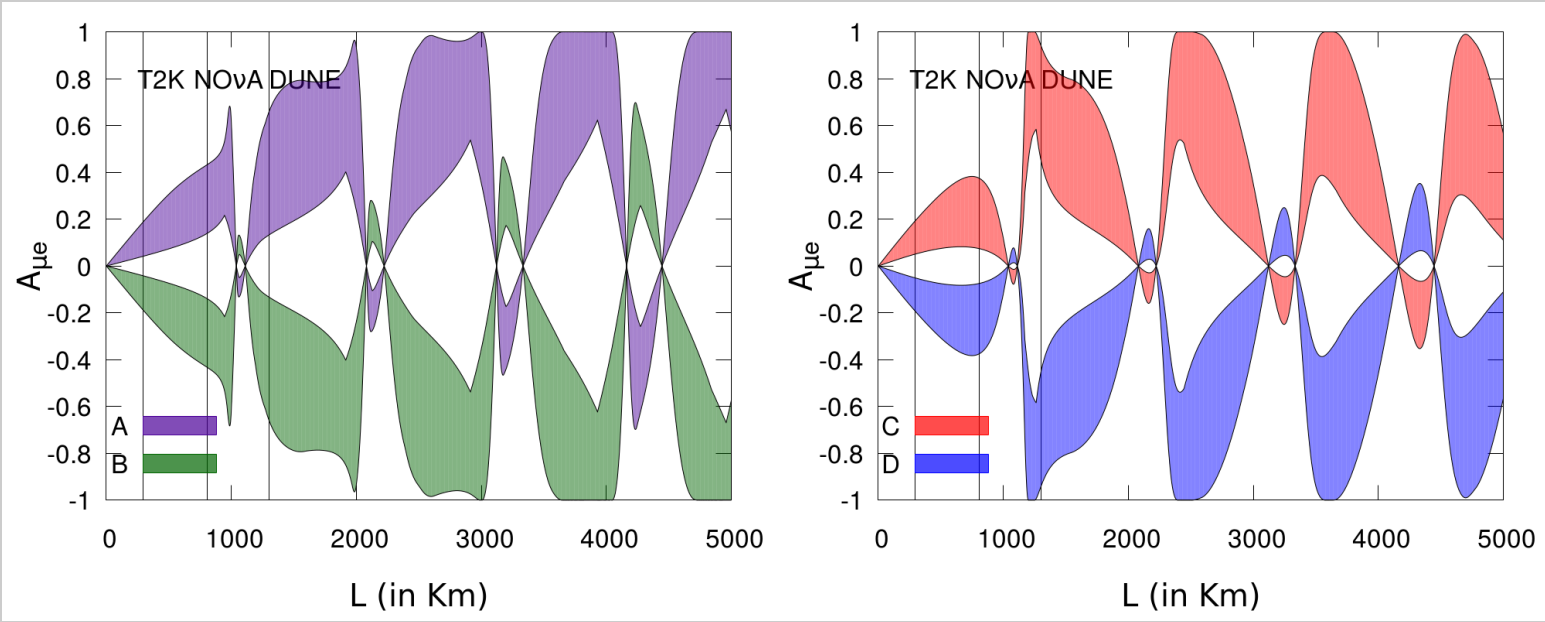

CP asymmetry parameter $A_{\mu e}$ vs. baseline length L for cases A,B,C,D.

1. For a fixed beam energy of $E = 1$GeV.

2. Plots are practically indistinguishable for NO and IO.

3. The bands are due to 3σ range θ_{23} while the other parameters are kept at their best fit values.

4. Experimental data should distinguish among the four cases and yield information on δ.

6. FLAVOR FLUX RATIOS AT NEUTRINO TELESCOPES

Source: Cosmic pp collisions (TeV-PeV)
$\rightarrow \pi^+\pi^- \rightarrow \mu^+\mu^-\nu_\mu\bar{\nu}_\mu \rightarrow e^+e^-2\nu_\mu 2\bar{\nu}_\mu\nu_e\bar{\nu}_e$

$$\Rightarrow \{\phi^S_{\nu_e}, \phi^S_{\bar{\nu}_e}, \phi^S_{\nu_\mu}, \phi^S_{\bar{\nu}_\mu}, \phi^S_{\nu_\tau}, \phi^S_{\bar{\nu}_\tau}\} = \phi_0\left\{\frac{1}{6}, \frac{1}{6}, \frac{1}{3}, \frac{1}{3}, 0, 0\right\}.$$

Source: Cosmic $p\gamma$ collisions (GeV-10^2GeV)
$\rightarrow \pi^+ \rightarrow \mu^+\nu_\mu \rightarrow e^+\nu_e + \bar{\nu}_\mu.$
$$\Rightarrow \{\phi^S_{\nu_e}, \phi^S_{\bar{\nu}_e}, \phi^S_{\nu_\mu}, \phi^S_{\bar{\nu}_\mu}, \phi^S_{\nu_\tau}, \phi^S_{\bar{\nu}_\tau}\} = \phi_0\left\{\frac{1}{3}, 0, \frac{1}{3}, \frac{1}{3}, 0, 0\right\}.$$

With $\phi^S_\ell \equiv \phi^S_{\nu_\ell} + \phi^S_{\bar{\nu}_\ell}$,

$$\{\phi^S_e, \phi^S_\mu, \phi^S_\tau\} = \phi_0\left\{\frac{1}{3}, \frac{2}{3}, 0\right\}$$

for both sources, ϕ_0 =overall normalization.

Flux at source $S \rightarrow$ flux at telescope T changed by neutrino oscillations averaged over many periods.

Effectively, $P(\nu_m \to \nu_\ell) = P(\bar{\nu}_m \to \bar{\nu}_\ell) \simeq \sum_i |U_{ei}|^2 |U_{mi}|^2$ and

$$\phi_\ell^T = \sum_i \sum_m \phi_m^S |U_{\ell i}|^2 |U_{mi}|^2 = \frac{\phi_0}{3} \sum_i |U_{\ell i}|^2 (|U_{ei}|^2 + 2|U_{\mu i}|^2).$$

It follows from the unitarity of U that
$\phi_\ell^T = \frac{\phi_0}{3}[1 + \sum_i |U_{\ell i}|^2 (|U_{\mu i}|^2 - |U_{\tau i}|^2)]$ which vanishes for exact $\mu\tau$ symmetry or antisymmetry, but is nonzero in general.

Neglect $\mathcal{O}(\sin^2\theta_{13}) \approx 0.01$ terms and define flavor flux ratios $R_e \equiv \phi_e(\phi_\mu + \phi_\tau)^{-1}$, $R_\mu \equiv \phi_\mu(\phi_e + \phi_\tau)^{-1}$, $R_\tau \equiv \phi_\tau(\phi_\mu + \phi_e)^{-1}$.
Now,

$$R_e \approx \frac{1 + \frac{1}{2}\sin^2 2\theta_{12}\cos 2\theta_{23} + \frac{1}{2}\sin 4\theta_{12}\sin 2\theta_{23} s_{13}\cos\delta}{2 - \frac{1}{2}\sin^2 2\theta_{12}\cos 2\theta_{23} - \frac{1}{2}\sin 4\theta_{12}\sin 2\theta_{23} s_{13}\cos\delta},$$

$$R_\mu \approx \frac{1 + \{c_{23}^2(1 - \frac{1}{2}\sin^2 2\theta_{12}) - s_{23}^2\}\cos 2\theta_{23} - \frac{1}{4}\sin 4\theta_{12}\sin 2\theta_{23} s_{13}\cos\delta(4c_{23}^2 - 1)}{2 - \cos^2 2\theta_{23} + \frac{1}{2}\sin^2 2\theta_{12}\cos 2\theta_{23} c_{23}^2 + \frac{1}{4}(3 - 4s_{23}^2)\sin 4\theta_{12}\sin 2\theta_{23} s_{13}\cos\delta},$$

$$R_\tau \approx \frac{1 + \{s_{23}^2(1 - \frac{1}{2}\sin^2 2\theta_{12}) + c_{23}^2\}\cos 2\theta_{23} - \frac{1}{4}\sin 4\theta_{12}\sin 2\theta_{23} s_{13}\cos\delta(4s_{23}^2 - 1)}{2 + \cos^2 2\theta_{23} + \frac{1}{2}\sin^2 2\theta_{12}\cos 2\theta_{23} c_{23}^2 + \frac{1}{4}(3 - 4c_{23}^2)\sin 4\theta_{12}\sin 2\theta_{23} s_{13}\cos\delta}.$$

Dependence on $\cos\delta$ makes R_ℓ double-valued except at $\theta = \pi/4$ ($\cos\delta = 0$ when $R_e = R_\mu = R_\tau = \frac{1}{2}$).

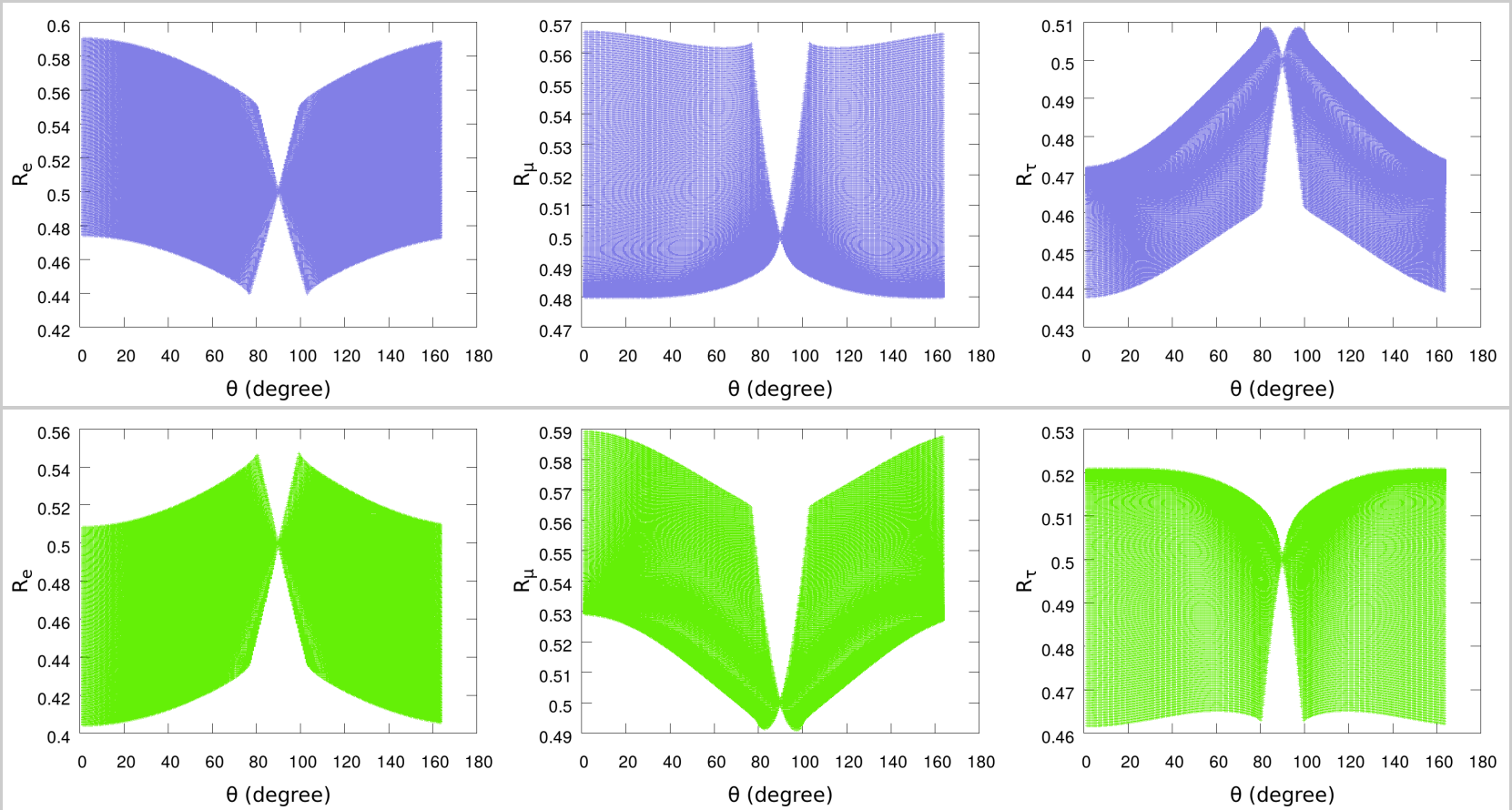

Flux ratios $R_{e,\mu,\tau}$ vs. θ for NO; range of θ: $12^\circ - 164^\circ$.
The upper (lower) panel corresponds to $\cos\delta \geq 0 (\leq 0)$.

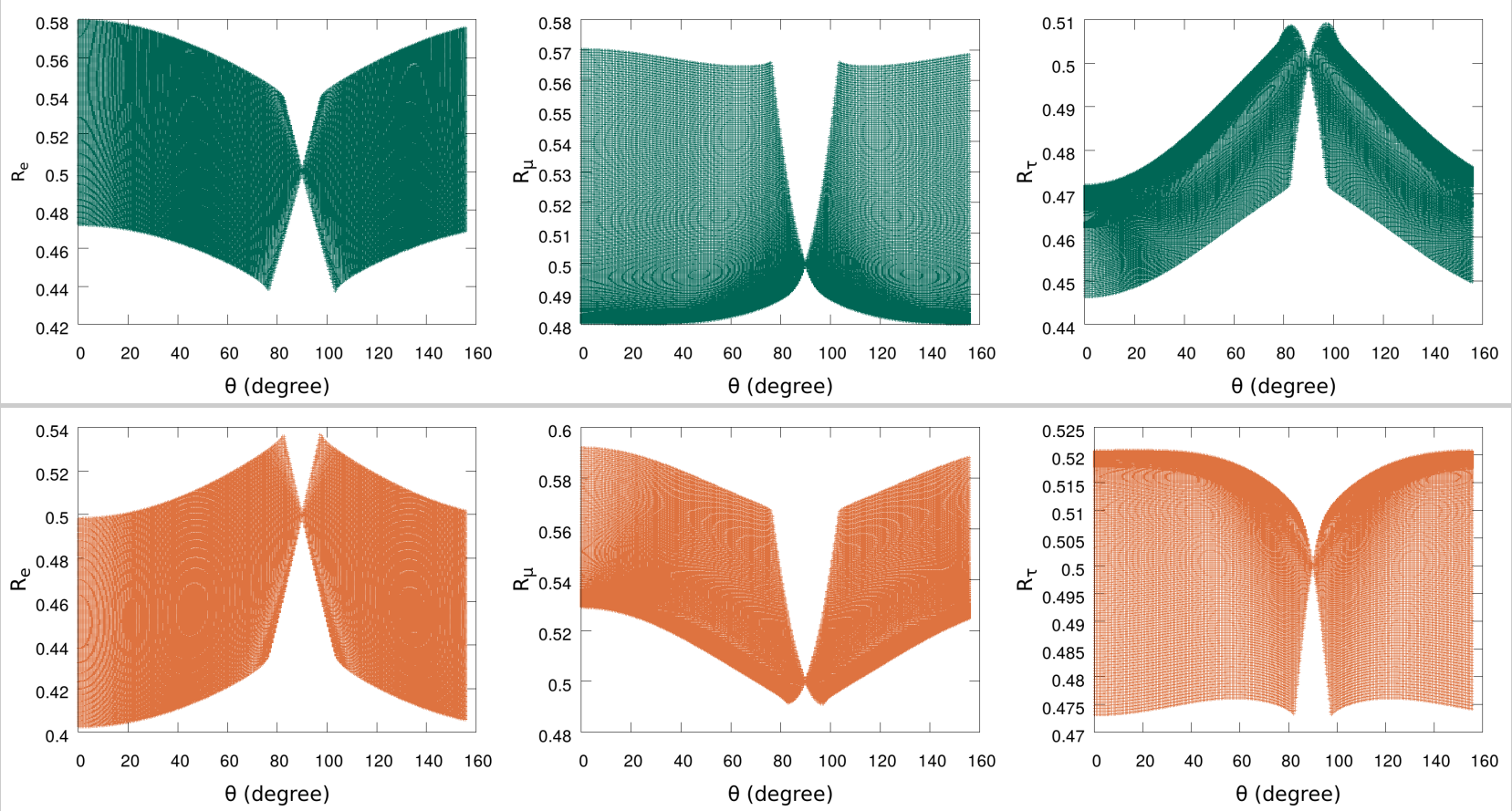

Flux ratios $R_{e,\mu,\tau}$ vs. θ for IO; range of θ: $2^\circ - 156^\circ$
The upper (lower) panel corresponds to $\cos\delta \geq 0 (\leq 0)$.

Continuous bands because of 3σ variation in input parameters.
Drastic change in R_e from 1/2 (as θ moves away from $\pi/2$) can be used to pinpoint θ.

7. CONCLUSIONS

- CP transformed mixed ν_μ-ν_τ antisymmetry in M_ν is proposed.
- With input neutrino neutrino mixing angles and mass-squared differences (3σ), ranges of values of neutrino masses for NO and IO given.
- Specific prediction on the $\beta\beta0\nu$ process to be tested crucially by nEXO.
- Neutrino CP asymmetry $A_{\mu e}$, when measured, should be able to provide information on the CP phase δ.
- Specific predictions on neutrino-antineutrino flavor flux ratios to be measured in neutrino telescopes.